

Abstract

Observations of in-situ generated atmospheric gravity waves associated with a stratospheric temperature enhancement (STE) are presented. Two sets of gravity waves are observed by molecular-aerosol lidar in conjunction with the early December 2000 STE event above Sondrestrom, Greenland. The first set of gravity waves shows downward phase progression with a vertical wavelength of ~ 8 km while the second set shows upward phase progression with a vertical wavelength of ~ 9 km. With estimates of the background wind fields from synoptic analyses, the various intrinsic gravity wave parameters of these two wave structures are found. The observed waves compare well to numerical modeling predictions, though the potential observation of a downward propagating wave would be unexpected.

1 Introduction

Stratospheric temperature enhancements (STEs) have been experimentally observed, theoretically and numerically modeled, and discussed in the scientific literature for some time, often under differing nomenclature which includes: stratospheric baroclinic zones, stratospheric sudden warmings (SSWs), winter stratospheric temperature anomalies, etc. SSW or a major warming is defined by the World Meteorological Organization as an increase in zonal-mean temperature of the polar region such that the net zonal-mean zonal winds become easterly north of 60° N at 10 hPa or below. An STE, such as the one discussed in this paper, leaves the lower stratosphere relatively undisturbed and is therefore considered distinct from an SSW. Meriwether and Gerrard (2004) have recently reviewed the phenomenology of STEs and have highlighted the scientific interest in the structures, including (1) the nature of their development and evolution, (2) how STEs may serve as precursors to sudden stratospheric warmings, and (3) the role of STEs as in-situ generators of middle atmospheric gravity waves. The first issue has been addressed by a number of authors, including a companion

Gravity waves generated during STEs

A. J. Gerrard et al.

Title Page

Abstract

Introduction

Conclusions

References

Tables

Figures



Back

Close

Full Screen / Esc

Printer-friendly Version

Interactive Discussion



paper by Thayer and Livingston (2008). This paper addresses the third issue by analyzing a unique STE event in December 2000, when the height of the stratopause dropped to ~ 42 km and temperatures were enhanced by ~ 50 K, described by Thayer and Livingston (2008).

As noted in the review by Meriwether and Gerrard (2004), numerical modeling of STE events by Fairlie et al. (1990) indicate the generation of gravity waves at the location of the STE. More recently, Fritts et al. (2006) and Vadas and Fritts (2001) have discussed strong temperature anomalies and subsequent local adjustment as potential generators of gravity waves. As reproduced in Fig. 1, upward propagating gravity waves are seen in model runs with horizontal wavelengths of ~ 1200 km, vertical wavelengths of ~ 8 km, and intrinsic periods of ~ 10 h. Though such large-scale waves do not individually transport large amounts of horizontal momentum vertically, their presence may nonetheless assist smaller-scale gravity waves towards convective or dynamical instability due to localized wave-wave interactions (Fritts and Alexander, 2003). Furthermore, it is not clear to what extent the associated localized momentum deposition plays a role in the re-stabilization of the high latitude middle atmosphere system (i.e., the reformation of the polar vortex) and return to geostrophy.

In-situ observations of STE-associated gravity waves have not been reported (Meriwether and Gerrard, 2004). To our knowledge, this paper presents the first direct, in-situ observations of gravity waves and associated wave structures generated during an STE event during 11–12 December 2000 above Sondrestrom, Greenland. The synoptic conditions of the STE observations were presented in Thayer and Livingston (2008); this study deals exclusively with the period of peak STE temperatures over Sondrestrom. In Sect. 2 we present a brief overview of the instrumentation and analysis, in Sect. 3 we discuss the gravity wave characteristics during the STE event, and in Sect. 4 we discuss these findings.

Gravity waves generated during STEs

A. J. Gerrard et al.

Title Page

Abstract

Introduction

Conclusions

References

Tables

Figures



Back

Close

Full Screen / Esc

Printer-friendly Version

Interactive Discussion



2 Instrumentation and analysis

Data used in this study originate in the ARCLITE molecular-aerosol lidar system located at Sondrestrom, Greenland. The ARCLITE system is discussed in detail in Thayer et al. (1997) and data from this system consist of range-time resolved temperature profiles of the upper stratosphere and lower mesosphere, relative gravity wave activity in the upper stratosphere, and aerosol volume backscatter coefficients. The data products have been used to explore mesospheric clouds (Thayer et al., 2003), relationship between gravity waves and mesospheric clouds (Gerrard et al., 1998, 2004a,b), thermal and gravity wave climatologies (Gerrard et al., 2000), and the synoptic development of the polar vortex (Gerrard et al., 2002). In Fig. 2 we present interpolated temperature profiles taken by the Sondrestrom lidar system in early December 2000 (Thayer and Livingston, 2008). Measurements were taken on the days indicated by black markers and interpolated across the entire duration of the STE event. Uncertainty on the lidar-deduced temperatures is less than 3 K below 70 km. Of particular note is the lidar data from 11–12 December (day of year 346–347), whose time evolution is also portrayed in Fig. 3. The temperature data here have been low pass filtered in the vertical with a cutoff at 7 km. Uncertainty on the measured temperatures is less than 5 K below 74 km. In these data the STE is clearly evident as a narrow ridge of temperatures exceeding 320 K; over 40 K above the climatological value (Gerrard et al., 2000).

From the ~25 h long set of molecular/aerosol lidar data spanning this time period, it is possible to obtain time-resolved relative atmospheric density perturbations between 30 km and 70 km as outlined in Gerrard et al. (1998, 2004b). The density perturbation data (relative to an estimated atmospheric background), available in 5 min by 192 m vertical resolution bins, have been low pass filtered with cutoffs at 2 km in the vertical and 30 min in the temporal. These relative density perturbations are shown in Fig. 3.

In a perturbation analysis of the base-state parameters of the ideal gas law, it can be shown that regions of high density perturbations correspond to regions of lower

Gravity waves generated during STEs

A. J. Gerrard et al.

Title Page

Abstract

Introduction

Conclusions

References

Tables

Figures

◀

▶

◀

▶

Back

Close

Full Screen / Esc

Printer-friendly Version

Interactive Discussion



temperatures. Such is the case on inspection of Figs. 2 and 3, where high density perturbations are 180° out of phase with the corresponding temperatures. As such, Figs. 2 and 3 essentially show the same thing, but gravity wave signatures are more readily extracted and analyzed in the relative density perturbations. From these figures, one sees that the STE peak temperature at ~ 42 km fluctuates by a few kilometers in height and in peak intensity through the course of the observations, presumably affected by the time-varying nature of the baroclinic zone and by other atmospheric structures, like gravity wave activity.

3 Gravity wave structures

Inspection of Fig. 3 shows at least two regions of relatively coherent wave-phase progression. These two areas of wave-like structure are highlighted in Fig. 3, where the waves in the upper left corner (centered at ~ -4 LST and ~ 65 km, red streaks) are referred to as “set 1”, and the waves on the right (centered at ~ 9 LST and ~ 50 km, blue streaks) are referred to as “set 2.” No wave structures were apparent below ~ 45 km.

Addressing set 1, the wave structure has a downward phase progression in time, a vertical wavelength of ~ 8 km and an observed period of ~ 5 h. This type of structure is commonly seen over Sondrestrom (for e.g., seen in data analyzed for Gerrard et al., 1998 and Gerrard et al., 2000), and has the characteristic of an atmospheric gravity wave propagating upwards in height (i.e., the phase progression is downward, which is indicative of upward energy progression). Strictly speaking, downward phase propagation results in upward propagation of energy in a fluid at rest or in a frame moving with the background wind. This would hold approximately true if the polar vortex mass did not move significantly during the STE event. Such an assumption is not unreasonable; for instance, analysis presented in Bhattacharya and Gerrard (2010) using stratospheric assimilated data from United Kingdom Met Office (UKMO) shows that geopotential height at 10 hPa remained relatively constant (~ 36 km) over Resolute Bay (75° N, 95° W) during the STE period reported here. Assimilated data from National

Gravity waves generated during STEs

A. J. Gerrard et al.

Title Page

Abstract

Introduction

Conclusions

References

Tables

Figures



Back

Close

Full Screen / Esc

Printer-friendly Version

Interactive Discussion



Gravity waves generated during STEs

A. J. Gerrard et al.

Title Page

Abstract

Introduction

Conclusions

References

Tables

Figures

◀

▶

◀

▶

Back

Close

Full Screen / Esc

Printer-friendly Version

Interactive Discussion



Center for Environmental Prediction (NCEP) gives the average horizontal wind velocity $\sim 50 \text{ m s}^{-1}$ at $\sim 65 \text{ km}$. If the wind velocity vector u is aligned with the gravity wave vector k (in general, gravity waves propagate in the direction of wind), and inferring the Brunt-Vaisala period from the nightly averaged temperature profile, the horizontal wavelength and intrinsic period of the wave can be estimated. The gravity wave dispersion relationship in this situation has two real roots. The first root, corresponding to the wave propagating in the direction of the background wind flow, results in a wave with a horizontal wavelength of $\sim 1700 \text{ km}$ and an intrinsic wave period of $\sim 10.5 \text{ h}$. The second root yields a wave propagating opposite the direction of the wind flow but with a horizontal wavelength of $\sim 400 \text{ km}$ and an intrinsic wave period of $\sim 4 \text{ h}$.

Addressing set 2, the wave structure has an upward phase progression in time, a vertical wavelength of $\sim 9 \text{ km}$, and an observed period of $\sim 26 \text{ h}$. Estimating that the background wind velocity from NCEP analyses to be $+70 \text{ m s}^{-1}$, coupled with the assumption of wave vector k approximately aligned with u , one obtains either an upward propagating gravity wave opposite the direction of the wind flow with a horizontal wavelength of $\sim 1870 \text{ km}$ and an intrinsic wave period of $\sim 10.4 \text{ h}$ or a downward propagating wave, also in the direction opposite of the wind flow, with a horizontal wavelength of $\sim 6200 \text{ km}$ and an intrinsic wave period of $\sim 12.6 \text{ h}$.

It can be shown that uncertainties of $\pm 1 \text{ km}$ in the vertical wavelengths, $\pm 1 \text{ h}$ in the observed periods, and $\pm 10 \text{ m s}^{-1}$ do not dramatically alter the estimated horizontal wavelengths and intrinsic periods.

4 Conclusions

Assuming that the first root of set 1 and the first root of set 2 are the physically meaningful roots, the observed gravity wave characteristics compare very well with model output of Fairlie et al. (1990). Furthermore, there was no indication of any wave structures below the STE temperature peak to indicate a gravity wave passing through the STE. As such, we conclude that this is an observation of upward propagating gravity waves generated in-situ by a STE event.

Gravity waves generated during STEs

A. J. Gerrard et al.

Title Page

Abstract

Introduction

Conclusions

References

Tables

Figures



Back

Close

Full Screen / Esc

Printer-friendly Version

Interactive Discussion



However, the second root of set 2, indicating a downward propagating gravity wave, poses an interesting possibility that warrants further investigation. No such waves were discussed within Fairlie et al. (1990), but given the ageostrophic dynamics of the baroclinic zone, the generation of a downward propagating gravity wave is not unreasonable. One would be inclined to think that the baroclinic nature of STE events, in an effort to return to geostrophy, would spawn gravity waves in the upper stratosphere and lower mesosphere that would be able to propagate both upwards and downwards. We are currently using ray-tracing methods to investigate the eventual result of gravity waves propagating (potentially) both upward and downward.

It should be noted that higher than normal total ozone content were reported in the Arctic vortex (till 63° N latitude for which ozone data was available) for the 2000–2001 winter; for December 2000, total ozone was higher by ~20 % compared to early 1980s (NCEP-NOAA Winter Bulletin, 2000–2001). An unusual and extensive ~3 km thick aerosol cloud layer, spanning almost the entire polar vortex around ~38 km altitude also formed in the first two weeks of December 2000, as reported by Gerding et al. (2003) observed from four different Arctic stations. Bhattacharya et al. (2004) have also reported increased gravity wave activity in the mesopause (hydroxyl airglow layer) polar vortex immediately following the STE events described in this paper. These observations in the current context increase the likelihood that the temperature enhancement, and the associated GW generation had their origin within a relatively shallow layer in the stratosphere. The long wavelength observed is also suggestive of a horizontally extensive forcing and a slower adjustment process (Fritts et al., 2006), unlike a vertically extended source typically found around the edges of a split vortex.

Based on this one observation, we are currently searching through the NCEP geopotential data archive for similar polar vortex configurations as those observed during this event. However, the combination of observing conditions, namely (a) the disruption of the polar vortex over Sondrestrom and actual occurrence of an STE when (b) there are clear sky conditions in which (c) the ARCLITE lidar system was collecting data is quite rare. Utilization of other lidar data archives, e.g., from the ALOMAR lidar system,

the Poker Flat Lidar system, and the Eureka lidar system, would likely increase the probability of observing gravity waves associated with a STE.

In conclusion, in-situ forcing of middle atmospheric gravity waves are of interest to the upper and lower atmospheric communities because, to date, little is known about the contribution that such waves may play in the global circulation. In this study we have demonstrated the likely origin of such in-situ forcing associated with an observed STE. Further studies are necessary to better understand the role of such waves in the high latitude environment, how frequently such waves are generated, and the synoptic impacts on the surrounding atmospheric environment.

Acknowledgements. The authors of this paper would like to thank site members of the Sondrestrom research facility and J. Livingston (SRI) for their support. AG and YB were supported in part by the National Science Foundation through ATM-0735452 and NSF-ATM-0457277.

References

- Bhattacharya, Y. and Gerrard, A. J.: Wintertime mesopause region vertical winds from Resolute Bay, J. Geophys. Res, 115, D00N07, doi:10.1029/2010JD014113, 2010. 14225
- Bhattacharya, Y., Shepherd, G. G., and Brown, S.: Variability of atmospheric winds and waves in the Arctic polar mesosphere during a stratospheric sudden warming, Geophys. Res. Lett., 31, L23101, doi:10.1029/2004GL020389, 2004. 14227
- Fairlie, T. D. A., Fisher, M., and O'Neill, A.: The development of narrow baroclinic zones and other small-scale structure during simulated major warmings, Q. J. Roy. Meteor. Soc., 116, 287–315, 1990. 14223, 14226, 14227, 14230
- Fritts, D. C. and Alexander M. J.: Gravity wave dynamics and effects in the middle atmosphere, Rev. Geophys., 41(1), 1003, doi:10.1029/2001RG000106, 2003. 14223
- Fritts, D. C., Vadas, S. L., Wan, K., and Werne, J. A.: Mean and variable forcing of the middle atmosphere by gravity waves, J. Atmos. Sol.-Terr. Phys., 68(3–5), 247–265, 2006. 14223, 14227
- Gerding, M., Baumgarten, G., Blum, U., Thayer, J. P., Fricke, K.-H., Neuber, R., and Fiedler, J.: Observation of an unusual mid-stratospheric aerosol layer in the Arctic: possible sources and

Gravity waves generated during STEs

A. J. Gerrard et al.

Title Page

Abstract

Introduction

Conclusions

References

Tables

Figures

◀

▶

◀

▶

Back

Close

Full Screen / Esc

Printer-friendly Version

Interactive Discussion



Gravity waves generated during STEs

A. J. Gerrard et al.

Title Page

Abstract

Introduction

Conclusions

References

Tables

Figures

◀

▶

◀

▶

Back

Close

Full Screen / Esc

Printer-friendly Version

Interactive Discussion

implications for polar vortex dynamics, *Ann. Geophys.*, 21, 1057–1069, doi:10.5194/angeo-21-1057-2003, 2003. 14227

Gerrard, A. J., Kane, T. J., and Thayer, J. P.: Noctilucent clouds and wave dynamics: Observations at Sondrestrom, Greenland, *Geophys. Res. Lett.*, 25, 2817–2820, 1998. 14224, 14225

Gerrard, A. J., Kane, T. J., and Thayer, J. P.: Year-round temperature and wave measurements of the arctic middle atmosphere for 1995–1998, in: *Geophysical Monograph Series 123: Atmospheric Science Across the Stratopause*, edited by: Siskind, D. E., Eckermann, S. D., and Summers, M. E., American Geophysical Union, Washington, D.C., 2000. 14224, 14225

Gerrard, A. J., Kane, T. J., Thayer, J. P., Duck, T. J., Whiteway, J. A., and Fiedler, J.: Synoptic-scale study of the arctic polar vortex's influence on the middle atmosphere: I. observations, *J. Geophys. Res.*, 107(D16), 4276, doi:10.1029/2001JD000681, 2002. 14224

Gerrard, A. J., Kane, T. J., Eckermann, S. D., and Thayer, J. P.: Gravity waves and mesospheric clouds in the summer middle atmosphere: A comparison of lidar measurements and ray modeling of gravity waves over Sondrestrom, Greenland, *J. Geophys. Res.*, 109(D10), D10103, doi:10.1029/2002JD002783, 2004a. 14224

Gerrard, A. J., Kane, T. J., Thayer, J. P., and Eckermann, S. D.: Concerning the upper stratospheric gravity wave and mesospheric cloud relationship over Sondrestrom, Greenland, *J. Atmos. Solar-Terr. Phys.*, 66, 229–240, 2004b. 14224

Meriwether, J. W. and Gerrard, A.: Mesosphere inversion layers and stratosphere temperature enhancements, *Rev. Geophys.*, 42(116), RG3003, doi:10.1029/2003RG000133. 2004. 14222, 14223

Thayer, J. and Livingston, J.: Observations of wintertime arctic mesospheric cooling associated with stratospheric baroclinic zones, *Geophys. Res. Lett.*, 35, L10109, doi:10.1029/2008GL034955, 2008. 14223, 14224, 14231

Thayer, J. P., Nielsen, N. B., Warren, R., Heinselman, C. J., and Sohn, J.: Rayleigh lidar system for middle atmosphere research in the arctic, *Opt. Eng.*, 36(7), 2045–2061, 1997. 14224

Thayer, J. P., Rapp, M., Gerrard, A. J., Gudmundsson, E., and Kane, T. J.: Gravity-wave influences on arctic mesospheric clouds as determined by a rayleigh lidar at Sondrestrom, Greenland, *J. Geophys. Res.*, 108(D8), 8449, doi:10.1029/2002JD002363, 2003. 14224

Vadas, S.-L. and Fritts, D.-C.: Gravity wave radiation and mean responses to local body forces in the atmosphere, *J. Atmos. Sci.*, 58, 2249–2279, 2001. 14223

Gravity waves generated during STEs

A. J. Gerrard et al.

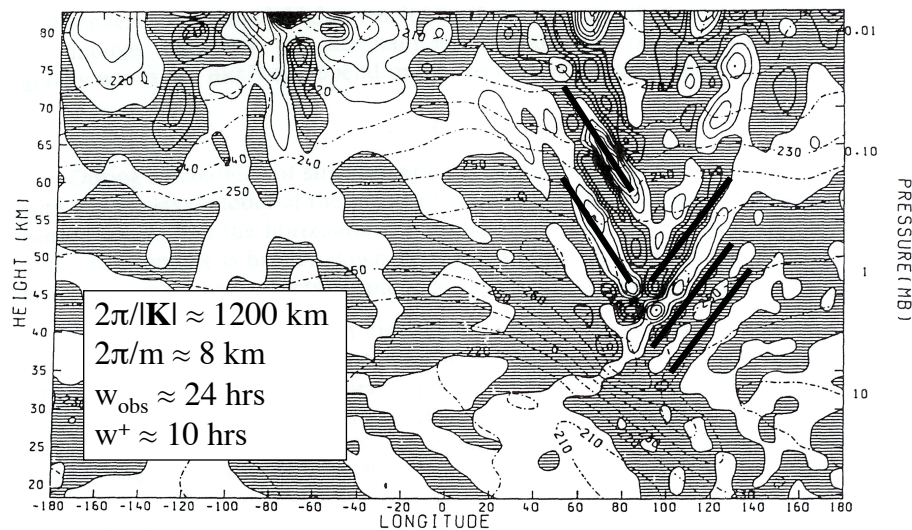


Fig. 1. From Fairlie et al. (1990). Simulated cross-section of temperature (dashed, units of K) and the divergence of the horizontal wind (solid, units of 10^{-6} s^{-1}) at 57.5°N on 25 February 1979. Regions of convergence are shaded. The figure has been modified to highlight modeled, upwardly propagating gravity waves to both the west and east of the STE/baroclinic zone. Estimated gravity wave parameters are listed.

Title Page

Abstract

Introduction

Conclusions

References

Tables

Figures

◀

▶

◀

▶

Back

Close

Full Screen / Esc

Printer-friendly Version

Interactive Discussion



Gravity waves generated during STEs

A. J. Gerrard et al.

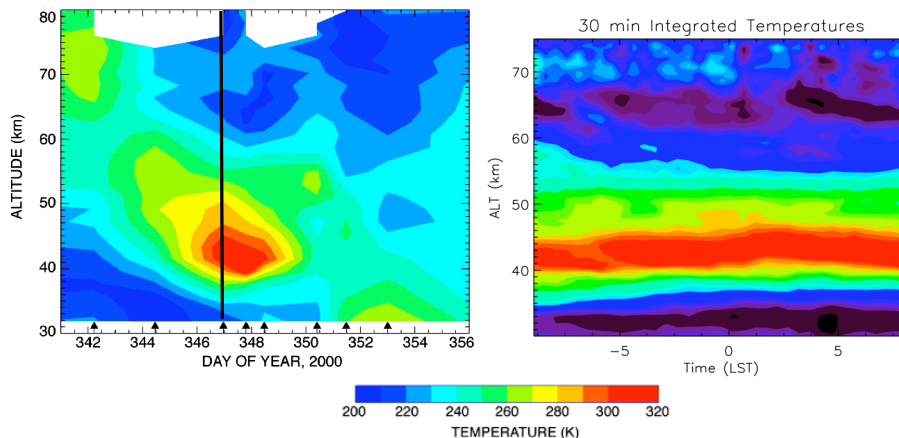


Fig. 2. From Thayer and Livingston (2008). Evolution of middle atmospheric temperatures over Sondrestrom, Greenland in December 2000 as measured by the molecular/aerosol lidar system. The vertical black line represents the day under study herein. (right) Range-time temperature evolution over Sondrestrom over the day near the estimated peak STE represented by the vertical black line (i.e., day of year 346–347, night of 11–12 December 2000, leap year). Time is local solar time (LST) with 0 representing midnight of 11 December.

Title Page

Abstract

Introduction

Conclusions

References

Tables

Figures

◀

▶

◀

▶

Back

Close

Full Screen / Esc

Printer-friendly Version

Interactive Discussion



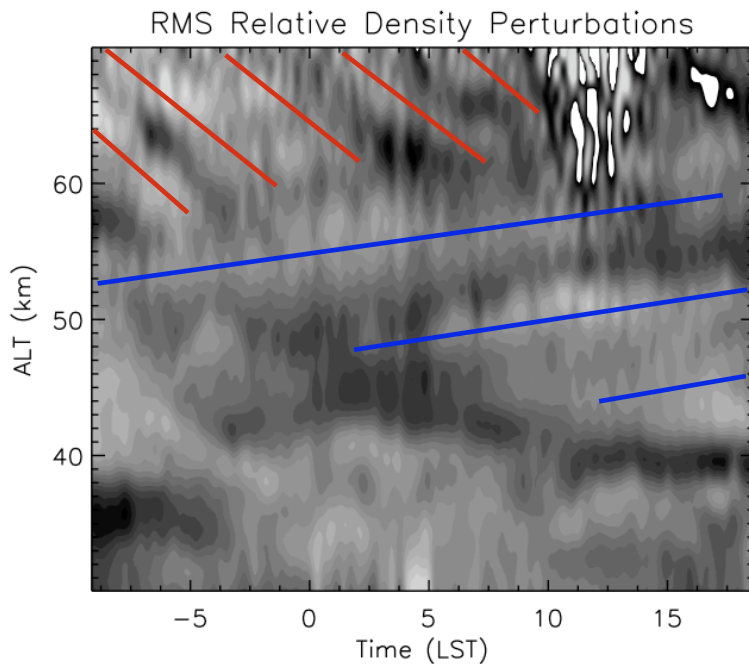


Fig. 3. Relative upper stratospheric and lower mesospheric density perturbations observed by the molecular/aerosol lidar system at Sondrestrom for the same range-time of Fig. 2. The relative density perturbations are scaled from -10% to 10% in 20 grey-scale intervals. Black represents the negative perturbations, while white represents the positive perturbations. Solar noise is present in the 60 km to 70 km region of the figures around 12 LST which prohibited robust calculation of the temperatures in Fig. 2. Phase peaks of upward and downward phase lines corresponding to the two gravity wave sets are highlighted.

Gravity waves generated during STEs

A. J. Gerrard et al.

Title Page

Abstract Introduction

Conclusions References

Tables Figures

◀ ▶

◀ ▶

Back Close

Full Screen / Esc

Printer-friendly Version

Interactive Discussion

